



ELSEVIER

Journal of Alloys and Compounds 300–301 (2000) 310–315

Journal of  
ALLOYS  
AND COMPOUNDS

www.elsevier.com/locate/jallcom

## Electron spin resonance and optical measurements of yttrium ortho-vanadate, doped with Nd<sup>3+</sup> ions

Ryszard Jablonski<sup>a</sup>, S.M. Kaczmarek<sup>b,\*</sup>, Marek Swirkowicz<sup>a</sup>, Tadeusz Lukasiewicz<sup>a,c</sup><sup>a</sup>*Institute of Electronic Materials Technology, 133 Wólczynska Str., 01-919 Warsaw, Poland*<sup>b</sup>*Institute of Optoelectronics, Military University of Technology, 2 Kaliski Str., 00-908 Warsaw, Poland*<sup>c</sup>*Institute of Applied Physics, Military University of Technology, 2 Kaliski Str., 00-908 Warsaw, Poland*

### Abstract

The electron spin resonance and optical properties of YVO<sub>4</sub> and YVO<sub>4</sub>:Nd<sup>3+</sup> crystals before and after ionizing radiation treatment with gamma quanta and electrons are presented. The obtained YVO<sub>4</sub> and YVO<sub>4</sub>:Nd<sup>3+</sup> (1 at. % Nd) single crystals show a lower content of point defects (growth defects, e.g. oxygen vacancies) and consequently, lower susceptibility to ionizing radiation in comparison to YAG: Nd<sup>3+</sup> crystals. Because of the angular dependence of the Nd<sup>3+</sup> resonance line position, we suppose the presence of structural defects like twins and mosaic structure. Moreover, for the first time the ESR spectrum of V<sup>4+</sup> in YVO<sub>4</sub> is reported. © 2000 Elsevier Science S.A. All rights reserved.

*Keywords:* Yttrium ortho-vanadate; Electron spin resonance; Optical measurements

### 1. Introduction

Yttrium orthovanadate single crystals doped with rare earth elements are very attractive laser material currently used for microlaser and diode laser pumped solid-state lasers. Physical properties make them superior to neodymium doped YAG [1–3].

It is a body centered tetragonal crystal with unit cell parameters  $a_0=b_0=7.118(0)$  Å,  $c_0=6.289(0)$  Å which belongs to the D<sub>4h</sub><sup>19</sup>-I<sub>1</sub>/amd space group [4]. The Nd<sup>3+</sup> ion is substituted for Y<sup>3+</sup> in the YVO<sub>4</sub> lattice. The nearest neighbours of the Nd<sup>3+</sup> ion in the structure are eight O<sup>2-</sup> ions.

Crystal-field parameters of Nd<sup>3+</sup> ions in GdVO<sub>4</sub> and YVO<sub>4</sub> were calculated by Anderson et al. [5]. Analysis of the ground term energy levels for Nd<sup>3+</sup> ions in YVO<sub>4</sub> were performed by Karayianis et al. [6]. Crystal field calculations and optical spectra measurements for Nd<sup>3+</sup> doped zircon-type YMO<sub>4</sub> laser hosts (M=V, P, As) were performed by Guillot et al. [7,8]. ESR measurements were reported by Rosenthal [9] who also gave spin-Hamiltonian parameters for Gd<sup>3+</sup> ion in YVO<sub>4</sub> lattice. Ranon [10] calculated data on Nd<sup>3+</sup>, Dy<sup>3+</sup>, Er<sup>3+</sup> and Yb<sup>3+</sup> ions in YVO<sub>4</sub>. Abraham et al. [11] measured Nd<sup>3+</sup>, Er<sup>3+</sup> and

Yb<sup>3+</sup> ion spectra in Yttrium and Lutetium Vanadates at helium temperature and of Gd<sup>3+</sup> at room temperature. Recently, Guillot et al. [12] have performed detailed measurements of Nd<sup>3+</sup> ions in YVO<sub>4</sub>, YAsO<sub>4</sub> and YPO<sub>4</sub>. Two types of Nd<sup>3+</sup> sites have been determined by ESR: undistorted sites and distorted sites.

In our work ESR and optical studies of undoped and neodymium doped YVO<sub>4</sub> crystals were performed in order to establish their structural and compositional quality. Moreover, the motivation of work has been to check if there are V<sup>4+</sup> or V<sup>3+</sup> ions in YVO<sub>4</sub> single crystals obtained in our laboratory.

### 2. Experiment

Single crystals of YVO<sub>4</sub>:Nd<sup>3+</sup> were grown in our laboratory by the Czochralski technique with use of an iridium crucible 50 mm in diameter and an active iridium afterheater. Stoichiometric charge material was prepared by mixing of Y<sub>2</sub>O<sub>3</sub> 5N from Aran Isles Chemicals Inc (USA), V<sub>2</sub>O<sub>5</sub> 4.5 N from Materials Technology Int.(USA) and Nd<sub>2</sub>O<sub>3</sub> 5 N from Kochlight (Germany). The obtained neodymium concentration was 1 at%.

The samples typically 3.5×3.5×2 mm<sup>3</sup> were measured in a Bruker ESP-300 ESR spectrometer (X-band). The spectrometer was equipped with a helium flow cryostat

\*Corresponding author. Tel.: +48-22-6859019; fax: +48-22-6668950.  
E-mail address: skaczmar@wat.waw.pl (S.M. Kaczmarek)

type ESR-900 Oxford Instruments. The ESR lines were observed in the temperature range from 4 K to 300 K. Absorption spectra were taken at a temperature of 300 K in the spectral range from 190 to 25 000 nm using Perkin-Elmer spectrophotometer (190–1100 nm) and a FTIR spectrometer (1400–25000 nm) before and after gamma irradiation. The as grown crystals were cut and polished into samples with approximate dimensions of 10 mm in diameter and 1 mm thick. According to transmission measurements the absorption ( $K$ ) and after a treatment, an additional absorption value, ( $\Delta K$ ), were calculated with use of the formula:  $\Delta K(\lambda) = 1/d \ln (T_1(\lambda)/T_2(\lambda))$  where  $\lambda$  is the wavelength,  $d$  is the sample thickness,  $T_1$  and  $T_2$  are the transmissions of the sample before and after an appropriate treatment procedure, respectively.

### 3. Results and discussion.

#### 3.1. ESR measurements.

Investigations of ESR spectra of  $\text{Nd}^{3+}$ ,  $\text{Gd}^{3+}$  and  $\text{V}^{4+}$  ions in  $\text{YVO}_4$  crystal were performed.

It should be noted that  $\text{Gd}^{3+}$  and  $\text{V}^{4+}$  were observed in undoped and  $\text{Nd}^{3+}$  doped crystals.

An angular dependence of ESR spectrum for a  $\text{YVO}_4$ : $\text{Nd}^{3+}$  sample at 4 K with the magnetic field rotated in the (010) plane is presented in Fig. 1. Also, in Fig. 1. spectra for  $\text{H} \parallel c$ ,  $\theta = 12^\circ$ ,  $\theta = 36^\circ$  and  $\text{H} \perp c$ , are shown. This ESR spectrum is isotropic when the magnetic field is rotated in the (001) plane. Two groups of eight hyperfine lines (hfs)

for  $I=7/2$  and one single strong line for  $I=0$  are observed. The linewidth of each hfs at 4 K for  $\text{H} \perp c$ -axis and, being equal to the peak-to-peak distance on the first derivative plot, is about 3.6 mT. With an increase of temperature the ESR spectrum intensity decreases. Above 30 K each hfs line broadens such that the resolved components are undetectable. The ESR spectrum disappears completely above 45 K as a consequence of rapid spin-lattice relaxation. The spectrum of  $\text{Nd}^{3+}$  ion in site with axial symmetry can be described by the following spin-Hamiltonian:

$$H = g_{\parallel} \beta H_z S_z + g_z \beta (H_x S_x + H_y S_y) + A_{\parallel} I_z S_z + A_z (I_x S_x + I_y S_y), \quad (1)$$

where  $S = 1/2$ ,  $I = 0$  for even-mass isotopes and  $I = 7/2$  for  $^{143}\text{Nd}$  and  $^{145}\text{Nd}$ ,  $A_{\parallel}$  and  $A_z$  are hfs constants and  $\beta$  is the Bohr magneton. The solid curve in Fig. 1 is calculated for the centre line ( $I=0$ ) according to the following relationship:

$$H_{\text{res}} = \nu / (g\beta/h); \quad g^2 = g_{\parallel}^2 \cos^2 \theta + g_z^2 \sin^2 \theta, \quad (2)$$

where  $\theta$  is an angle between the direction parallel to the  $c$ -axis and magnetic field,  $\nu$ -microwave frequency,  $h$  the Planck constant,  $g_{\parallel}$  and  $g_z$  are listed in Table 1.

The spectra presented in Fig. 1 for different angles are probably a result of overlapping of two or three spectra connected with twins (it is clearly seen for  $\theta = 12^\circ$ ). Simultaneously, as magnetic field is rotated from the  $a$  ( $\theta = 90^\circ$ ) to the  $c$  ( $\theta = 0^\circ$ ) direction, each hyperfine and central line broadens such that the resolved components

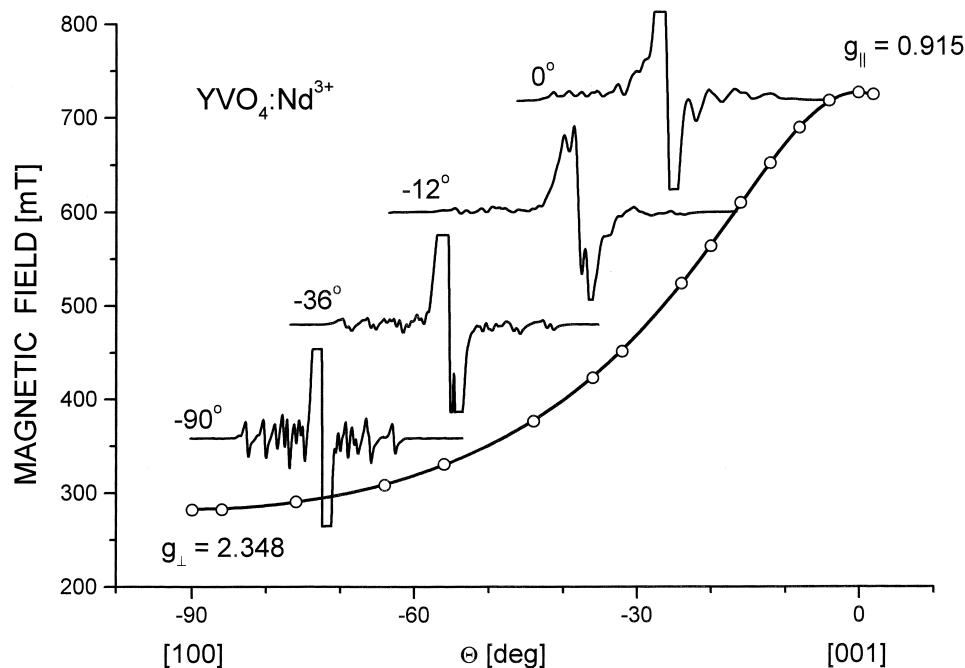


Fig. 1. Angular dependence of ESR lines at 4 K of  $\text{YVO}_4$ : $\text{Nd}^{3+}$  with magnetic field in (010) plane. Circles, experimental results; solid line, results calculated according to Eq. (2).

Table 1  
Spin-Hamiltonian parameters of  $\text{Nd}^{3+}$  in  $\text{YVO}_4$

| $g_{\parallel}$ | $g_z$    | Isotope | $10^{-4}\text{cm}^{-1}$ |          | Ref.      |
|-----------------|----------|---------|-------------------------|----------|-----------|
|                 |          |         | $A_{\parallel}$         | $A_z$    |           |
| 0.9132          | 2.35     | 143     | 119.5(2)                | 259(1)   | [10]      |
|                 |          | 145     | 74.3(1)                 | 159(2)   |           |
| 0.915(5)        | 2.348(2) | 143     | –                       | 261.2(2) | This work |
|                 |          | 145     | –                       | 162.2(2) |           |

are undetectable at the  $\text{H}||\text{c}$ -axis. The broadening can be explained by the existence of a mosaic structure.

Apart from the ESR of neodymium spectrum in all our  $\text{YVO}_4$  single crystals in the whole measurement range from 6 K to 300 K, the  $\text{Gd}^{3+}$  spectrum is observed with an intensity ratio  $\text{Gd}^{3+}/\text{Nd}^{3+} = 0.0005$  (at temperature 20 K). Moreover, the  $\text{Gd}^{3+}$  spectrum is also observed for undoped single crystals.

Resonance transitions of  $\text{Gd}^{3+}$  can be described by the following spin-Hamiltonian:

$$\mathbf{H} = g\beta\mathbf{HS} + B_2^0O_2^0 + B_4^0O_4^0 + B_6^0O_6^0 + B_4^4O_4^4 + B_6^4O_6^4,$$

Where  $\mathbf{H}$  is intensity of magnetic field,  $\mathbf{S}$  is the spin vector of the  $\text{Gd}^{3+}$  ion ( $S=7/2$ )  $B_m^n$  are experimental parameters,  $O_m^n$  are spin operators in the notation of Abragam and Bleaney [11].

In Fig. 2 ESR spectrum of  $\text{Gd}^{3+}$  for  $\text{H}||\text{c}$  at temperature 300 K for nominally undoped  $\text{YVO}_4$  specimen is depicted. In the same figure, as an example one line is enlarged to show hfs lines. Such a structure is observed for all  $\text{Gd}^{3+}$  lines. The linewidth  $\Delta H_{\text{pp}}$  of all lines for  $\text{H}||\text{c}$  is equal to

Table 2  
 $b_2^0=3 B_2^0$ ,  $b_4^n=60 B_4^n$ ,  $b_6^n=1260 B_6^n$ ,  $n=0, 4$  [in  $\text{cm}^{-1} 10^{-4}$ ]

| Parameters | This work          | [9]                 |
|------------|--------------------|---------------------|
| $g$        | $1.9880 \pm 0.005$ | $1.9916 \pm 0.0002$ |
| $b_2^0$    | $-439.5 \pm 2$     | $-441.6 \pm 0.2$    |
| $b_4^0$    | $-1.21 \pm 0.02$   | $-1.5 \pm 0.1$      |
| $b_6^0$    | $0.464 \pm 0.008$  | $+0.8 \pm 0.6$      |
| $b_4^4$    | $37.1 \pm 2$       | $+8.3 \pm 0.1$      |
| $b_6^4$    | 0.0                | $0.0 \pm 0.2$       |

0.5 mT. For  $\text{YVO}_4$  specimens doped with neodymium the  $\text{Gd}^{3+}$  linewidth changes and the value for different lines are presented in round brackets in Fig. 2. Taking into account only diagonal terms of the spin-Hamiltonian for  $\text{H}||\text{c}$  the following relations are obtained:

$$\pm 7/2 \rightarrow 5/2 H_{\text{res}} = H_0 + (6b_2^0 + 20b_4^0 + 6b_6^0)$$

$$\pm 5/2 \rightarrow 3/2 H_{\text{res}} = H_0 + (4b_2^0 - 10b_4^0 - 14b_6^0)$$

$$\pm 3/2 \rightarrow 1/2 H_{\text{res}} = H_0 + (2b_2^0 - 12b_4^0 + 14b_6^0)$$

$$+ 1/2 \rightarrow -1/2 H_{\text{res}} = H_0$$

with an intensity ratio 7:12:15:16:15:12:7.

According to Table 2  $b_4^0$  and  $b_6^0$  parameters can be omitted, therefore broadening of lines depends mainly on  $b_2^0$  parameter. An increase of  $\text{Gd}^{3+}$  linewidth in  $\text{Nd}^{3+}$  doped single crystal in comparison to undoped crystal is equal to 1.3, 0.8, 0.35, 0.16, 0.46, 0.94, 1.35 mT for different lines which corresponds to  $b_2^0$  change  $\Delta b_2^0 = 0.2$  mT ( $1.858 \cdot 10^{-4} \text{cm}^{-1}$ ); it is equivalent to about 0.4%. The

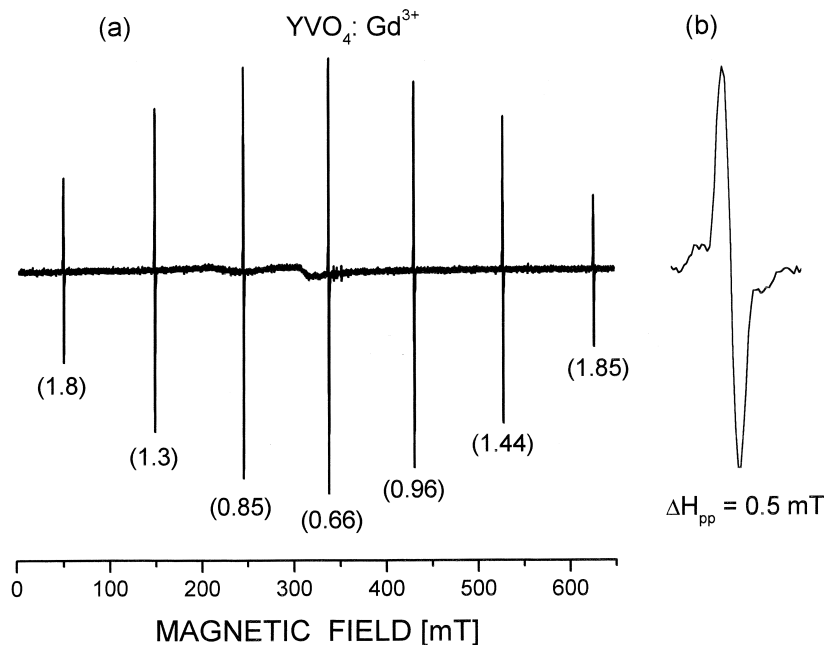


Fig. 2. (a) ESR spectrum of  $\text{Gd}^{3+}$  ions in nominally undoped crystal. Numbers in brackets denote linewidths for specimens doped with 1at%  $\text{Nd}^{3+}$ . (b) Hyperfine splitting in the central transition. The outer lines correspond to the odd isotopes; lines are not clearly resolved.

broadening of  $Gd^{3+}$  lines for  $Nd^{3+}$ -doped single crystals can be explained by changes in the  $b_m^n$  parameters, and especially in  $b_2^0$ . Probably it is connected with a mosaic structure which is formed during growth of a doped single crystal.

In the ESR spectrum for  $H||c$ -axis at temperatures between 6 and 40 K eight-line hyperfine pattern is observed with a splitting of about 12.2 mT which is a result of interaction with the  $V^{4+}$  nucleus ( $I=7/2$ , abundance = 100%). This hyperfine pattern is depicted in Fig. 3 in detail. Vanadium should enter to the  $YVO_4$  lattice as a  $V^{5+}$  ion. But, during the crystal growth process  $V^{4+}$  and  $V^{3+}$  ions can be also generated [13–15]. In our case, the intensity of lines which we suppose are related to the presence of  $V^{4+}$  ions are at least one order of magnitude lower than for the  $Gd^{3+}$  ion. After heat treatment in air at a temperature 1000°C for 5 h this spectrum completely disappears which means that transition  $V^{4+} \rightarrow V^{5+}$  take place due to removal of oxygen vacancies.

### 3.2. Absorption measurements

Fig. 4 presents absorption spectrum of Nd doped  $YVO_4$  single crystal for all transitions from  $^4I_{9/2}$  manifold (ground state) in the range 200–800 nm in comparison to Nd doped YAG. Fundamental absorption edge (FAE) is about 340 nm. The ratio of the absorption of  $YVO_4:Nd$

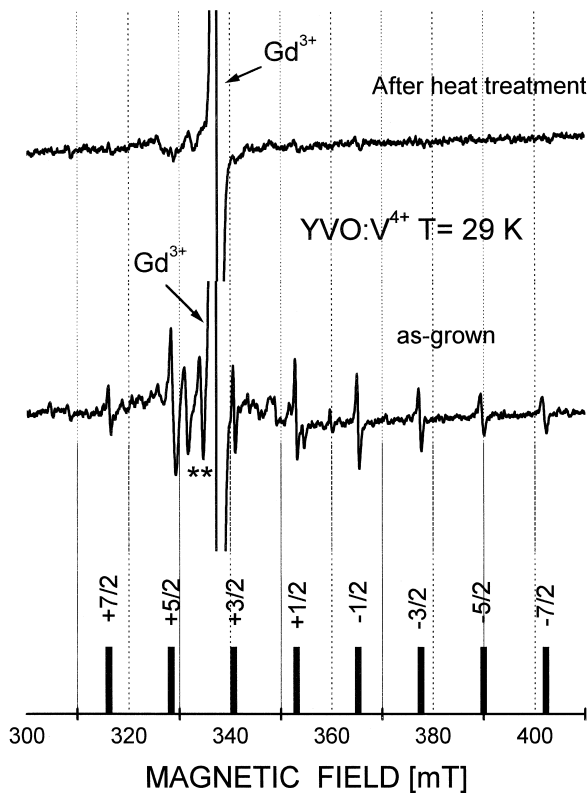


Fig. 3. ESR spectra of  $V^{4+}$  ions for  $H||c$  at 29 K for as-grown crystal and after heat treatment in air 1000°C for 5 h. \* non identified lines.

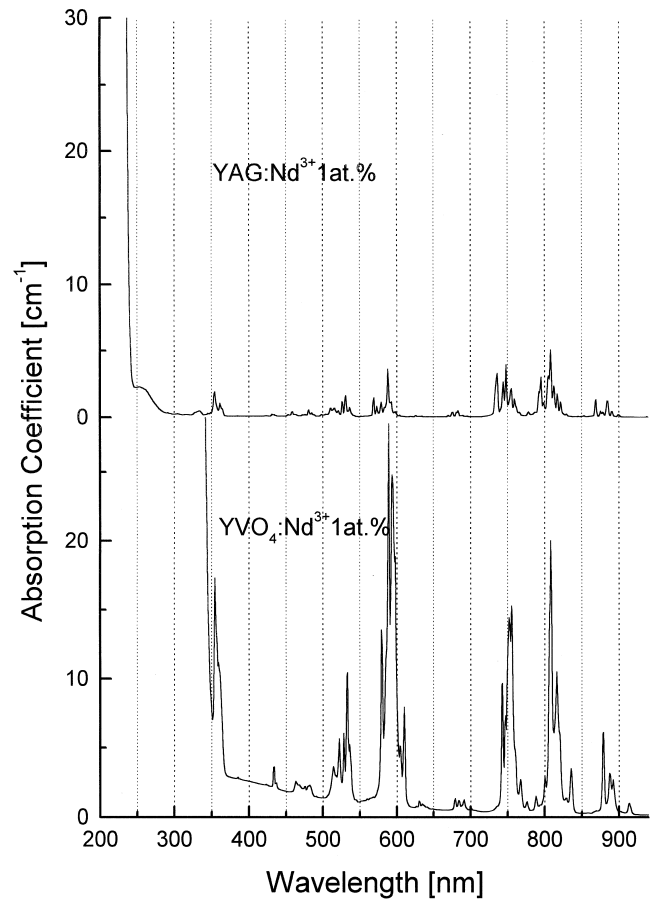


Fig. 4. Absorption of Nd doped  $YVO_4$  single crystal at 300 K in comparison to YAG one.

with respect to YAG: Nd for  $\lambda = 808$  nm is as high as 4. An increase of absorption with a decrease of wavelength which is observed for small wavelengths is probably connected with accuracy of surface polishing of samples.

After gamma irradiation of  $YVO_4$  and  $YVO_4:Nd$  crystals two bands arise in absorption spectrum with maxima at 380 and 556 nm. They are depicted in Fig. 5 for undoped  $YVO_4$  (Fig. 5a) and  $YVO_4:Nd$  (Fig. 5b) single crystals for two doses of  $\gamma$ -quanta:  $10^5$  Gy (curve 1) and  $10^6$  Gy (curve 2). The bands are similar to those for YAG but their intensity is much lower. Narrow intensive lines observed in Fig. 5b for additional absorption in  $YVO_4:Nd$  crystal are connected with the presence of narrow intensive Nd lines in absorption spectrum of the crystal. Small shift of absorption lines in the wavelength scale gives such large values of additional absorption.

In summary, in  $YVO_4$  crystal the density of point defects (shape and intensity of additional absorption bands) is lower than in YAG; the  $YVO_4$  crystals show absence of absorption due to non-controlled  $Fe^{3+}$  impurity (optically active).

Irradiations with gamma rays performed with greater doses ( $10^6$  Gy-curves indicated as 2 in Fig. 5a and b) show that further increase in absorption value is not observed for

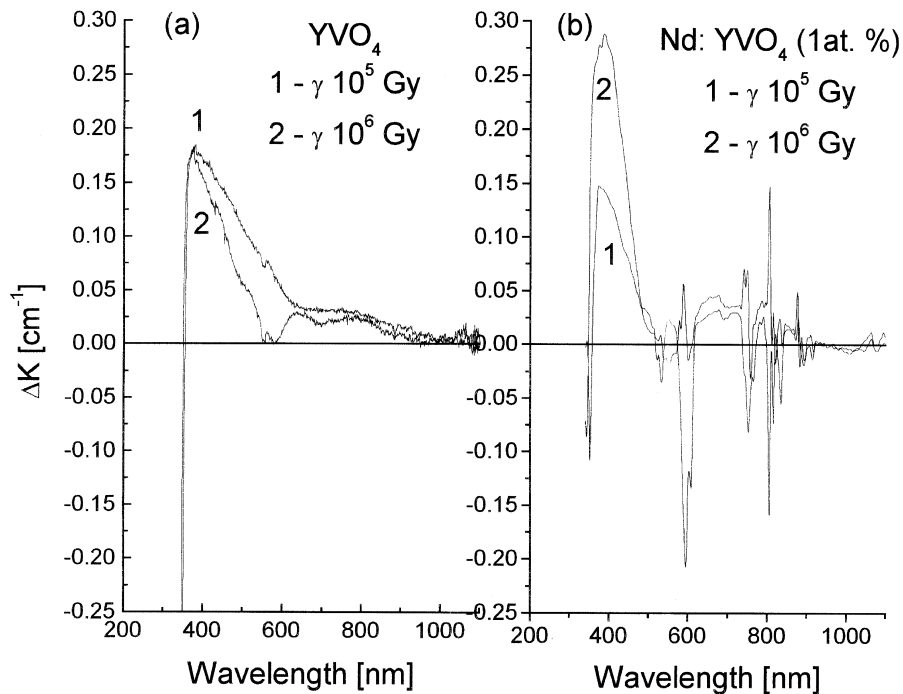


Fig. 5. Additional absorption in  $\text{YVO}_4:\text{Nd}^{3+}$  crystals after gamma irradiation..

undoped  $\text{YVO}_4$  crystals. For Nd doped  $\text{YVO}_4$  crystals, doubling of intensity of additional absorption after gamma irradiation with a dose of  $10^6$  Gy with respect to  $10^5$  Gy is seen. Therefore, it can be concluded that saturation takes place for doses such high as  $10^5$  Gy applied to undoped  $\text{YVO}_4$  single crystals (all point defects undergo recharging process), while for  $\text{YVO}_4:\text{Nd}$  such phenomenon does not take place. Usually additional absorption of rare-earth doped single crystals is lower than for undoped ones. Such behaviour of additional absorption of  $\text{YVO}_4:\text{Nd}$  single crystal suggests the presence of more defected structures in

this crystal. It may be some type of structural defect. They are also seen in luminescence spectrum, where changes in relative intensities interstices are observed after gamma irradiation Fig. 6.

#### 4. Conclusions

Undoped  $\text{YVO}_4$  and Nd doped  $\text{YVO}_4$  single crystals obtained in our laboratory exhibit good optical quality and strong absorption in the range of diode laser pumping

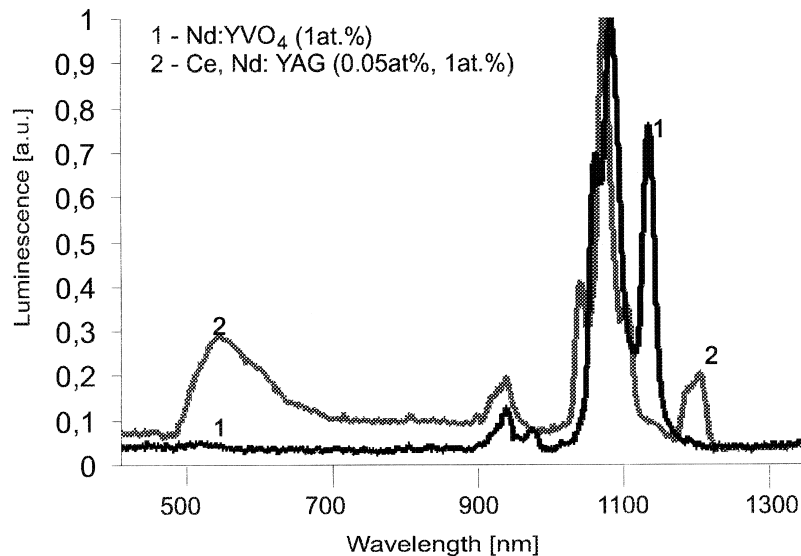


Fig. 6.  ${}^4\text{F}_{3/2} \rightarrow {}^4\text{I}_{11/2}$  photoluminescence spectrum for  $\text{YVO}_4:\text{Nd}^{3+}$  at 300 K.

(about  $19 \text{ cm}^{-1}$  in the range 750–850 nm). These crystals show lower susceptibility to gamma and electron irradiations in comparison to YAG. From additional absorption after  $\gamma$ -irradiation, ESR and radioluminescence measurements it can be concluded that there exist structural defect in  $\text{YVO}_4:\text{Nd}^{3+}$  single crystal around Nd lattice positions resulting in emission damping of Nd ions. The splitting of neodymium line observed in ESR spectrum is probably connected with an existence of twins in the specimens. The broadening of  $\text{Nd}^{3+}$  and  $\text{Gd}^{3+}$  lines for [001] direction suggests, on the other hand, an existence of mosaic structure in the sample. In the specimens under examination gadolinium atoms clearly have existed as an impurity with rather low concentration. It should be mentioned that gamma irradiation has no influence on ESR spectra of undoped and Nd doped  $\text{YVO}_4$  crystals.

Moreover, according to ESR measurement  $\text{V}^{4+}$  ions are present in  $\text{YVO}_4$  crystals. Their existence can be connected with oxygen vacancies which are formed during crystal growth in the nitrogen atmosphere. The concentration of  $\text{V}^{4+}$  ions is also very low, even lower than of  $\text{Gd}^{3+}$ . This work is in progress.

## References

- [1] D.G. Matthews, J.R. Boon, R.S. Conroy, B.D. Sinclair, *J. Mod. Opt.* 43 (1966) 1079.
- [2] B.H.T. Chai, G. Loutts, J. Lefaucheur et al., *OSA Proceedings on Advanced Solid-State Lasers* 20 (1994) 41.
- [3] T. Taira, A. Mukai, Y. Nozava, T. Kobayashi, *Opt. Lett.* 16 (1991) 1955.
- [4] B.C. Chakoumakos, M.M. Abraham, L.A. Boatner, *J. Solid State Chem.* 109 (1994) 197–202.
- [5] F.G. Anderson, P.L. Summers, H. Weidner, P. Hong, R.E. Peale, *Phys. Rev. B* 50 (20) (1994-II) 14802–14808.
- [6] N. Karayianis, C.A. Morrison, D.E. Wortman, *J. Chem. Phys.* 62 (10) (1975) 4125–4129.
- [7] O. Guillot-Noel, A. Kahn-Harari, B. Viana, D. Vivien, E. Antic-Fidancev, P. Porcher, *J. Phys.: Condens. Matter* 10 (1998) 6491–6503.
- [8] O. Guillot-Noel, A. Kahn-Harari, B. Viana, D. Vivien, E. Antic-Fidancev, P. Porcher, *J. Alloys Comp.* 177 (1998) 275–277.
- [9] J. Rosenthal, *Phys. Rev.* 164 (1967) 363.
- [10] U. Ranon, *Phys. Lett.* 28A (3) (1968) 228–229.
- [11] M.M. Abraham, B. Bleaney, J.Z. Pfeffer, *Appl. Magn. Reson.* 14 (1998) 393–396.
- [12] O. Guillot-Noël, D. Simons, D. Gourier, *J. Phys. Chem.* 60 (1999) 555–565.
- [13] T. Katsumata, H. Takashima, T. Michino, Y. Nobe, *Mat. Res. Bull.* 29 (12) (1994) 1247–1254.
- [14] S. Erdei, *J. Cryst. Growth* 134 (1993) 1.
- [15] S. Erdei, G.G. Johnson, F.W. Ainger, *Cryst. Res. Technol.* 29 (1994) 815.